Eigenvalue Problems, Jacobi's method and its Application to Differential Equations Describing Physical Problems

René Ask, Kaspara Skovli Gåsvær & Maria Linea Horgen
(Dated: September 30, 2019)

We study a method for solving a ordinary differential equations (DEs) that present themselves as eigenvalue problem. These are approximated as eigenvalue matrix equations and solved using Jacobi's method. We benchmark the implementation by computing its time used and its convergence rate as functions of number of grid points. We further apply the method to three different DEs: the classical Buckling Beam problem, and the radial equation of the Schrödinger equation for a 3D harmonic oscillator with one and two electrons.

We find that the time used by Jacobi's method is substantially slower than that of the optimized eigenvalue solver *eig_sym* available from Armadillo. We further study the rate of convergence as a function of number of grid points which confirms the predicted relationship found in the literature. We present a numerical result on the relative error of the computed eigenvalues and find a proportionality relation as function of number of grid points.

We demonstrate broad agreement between the computed eigenvalues using Jacobi's method and the predicted analytical values either derived in this article or found in the literature. We discuss the difficulties with respect to choosing the parameters involved by the imposed Dirichlet boundary conditions that arise from solving the radial equation of the 3-dimensional harmonic oscillator potential. As a final check of our implementation, we study the probability distributions of ground state wavefunctions for several different parameters and find that their behaviour agree with predictions. As a final remark, we conclude that our implementation is not particularly efficient. Unless optimized, one is better off using another method to compute the spectra or use fast eigenvalue solvers such as *eig_sym*.

I. INTRODUCTION

Ordinary differential equations (DEs) show up in all branches of physics, and since only a subset of these allow closed-form solutions, applying approximation schemes of various kinds is necessary to solve more complicated problems that fundamentally model a given natural phenomenon more accurately than what models that display closed-form solutions can. Many such DEs are eigenvalue problem to begin, usually written in with respect to some continuous basis. Physical processes that can be described by a finite-dimensional vector space naturally fall into the scheme of matrix equations and techniques developed for handling such equations can easily be applied, but DEs involve continuous functions that require an infinite-dimensional vector space to describe the solution spaces. However, by paying a small price in the form of loss of accuracy, we can approximate the solutions to DEs by discretization in a way that recasts the DE into a matrix equation of the form $A\boldsymbol{x} = \lambda\boldsymbol{x}$. A small price to pay for salvation, indeed, for at this point we can apply techniques developed to solve such eigenvalue problems. Conceptually, we can think of this as defining a mapping that maps the differential operator acting on an infinite Hilbert space onto an approximate operator represented as a matrix. We then solve the eigenvalue equation involving this approximated operator instead.

In this report we explore Jacobi's method for solving such eigenvalue problems. We look at three physical problems modelled by DEs as described above: *The Buckling Beam problem* and *Quantum dots in three dimensions* for both one and two interacting electrons. The overarching goal being to look at how one simple method applies to several physical problems because these all display similarities that allows them to be recast into eigenvalue problems involving Toeplitz matrices. We first develop an algorithm to solve arbitrary eigenvalue equations involving symmetric matrices by implementation of Jacobi's method, which we then use to find the eigenvalues of the resulting eigenvalue problem. We develop several unit test to make sure that our algorithm runs correctly and preforms the proper mathematical calculations while preserving some important mathematical properties. Since these physical problems inherently involve quantities with units, we scale the equations such that our solution methods easily apply. As a measure of performance, we shall benchmark Jacobi's method against a well known eigenvalue solver for symmetric matrices from Armadillo[1].

Finally, for codes used to produce the results in this article and their documentation, see [2]

II. METHOD

A. Discretization

We study here a second order differential equation on the general form

$$-\frac{\mathrm{d}^2u(\rho)}{\mathrm{d}\rho^2} + V(\rho)u(\rho) = \lambda u(\rho). \tag{1}$$

Discretization of this leads to

$$-\frac{u_{i+1}-2u_i-u_{i+1}}{h^2}+V_iu_i=\lambda u_i, \tag{2}$$

where $u_i \equiv u(\rho_i)$ and $\rho_i \equiv \rho_0 + ih$ for some step size h. Furhermore we assume a particular type of Dirichlet boundary condition, $u_0 = u_{n+1} = 0$. Eq. (2) is equivalent with the eigenvalue problem

$$\frac{1}{h^2}\begin{bmatrix} U_1 & -1 & 0 & \cdots & 0 \\ -1 & U_2 & -1 & \cdots & 0 \\ 0 & -1 & U_3 & \cdots & 0 \\ \vdots & \vdots & \vdots & \ddots & \vdots \\ 0 & 0 & \cdots & -1 & U_n \end{bmatrix}\begin{bmatrix} u_1 \\ u_2 \\ \vdots \\ u_{n-1} \\ u_n \end{bmatrix} = \lambda \begin{bmatrix} u_1 \\ u_2 \\ \vdots \\ u_{n-1} \\ u_n \end{bmatrix}, \tag{3}$$

with

$$U_i \equiv 2 + V_i.$$

Formally, we're approximating the spectrum of the differential operator acting on an infinite-dimensional Hilbert space in eq. (1) by the spectrum of the finite-dimensional matrix in eq. (3). One might think this is a restrictive definition to go by, but all functions studied in this article are solutions to problems that modell physical processes and must be required to obey

$$\int |f|^2 d\mu < \infty. \tag{4}$$

B. A Buckling Beam problem

We commence by studying the classical problem of a buckling beam whose process is described by

$$-\gamma\frac{\mathrm{d}^2u(x)}{\mathrm{d}x^2} = Fu(x), \tag{5}$$

which essentially is a 1-dimensional wave equation. Assume here that $x \in [0, L]$ for some known length L, γ is a material constant and suppose we know the exact value of F. Defining a new variable $\rho \equiv x/L$, we can rewrite the DE as

$$-\frac{\mathrm{d}^2u(\rho)}{\mathrm{d}\rho^2} = \frac{FL^2}{\gamma}u(\rho) \equiv \lambda u(\rho), \tag{6}$$

where $\rho \in [\rho_0, \rho_N] = [0, 1]$. Imposing the boundary conditions $u(0) = u(1) = 0$, one obtains the eigenvalue spectrum

$$\lambda_n = \pi^2 n^2, \qquad n = 0, 1, 2, ..., \tag{7}$$

see section VI A for the derivation. Eq. (6) can easily be recast into eq. (3) with $U_i = 2\ \forall i \in \{1, 2, ..., n\}$.

C. Quantum dots in 3D - one electron

In this section, we'll study Schrödinger's equation for one electron. The radial equation of any spherically symmetric potential $V(r)$ can be written as

$$-\frac{\hbar^2}{2m}\frac{\mathrm{d}^2u(r)}{\mathrm{d}r^2}+\left[V(r)+\frac{\hbar^2}{2m}\frac{\ell(\ell+1)}{r^2}\right]u(r) = Eu(r), \tag{8}$$

where the radial function $R(r)$ is related to the eq. (8) by the definition $u(r) \equiv rR(r)$, and $r \in [0, \infty)$[5]. In this article we'll restrict ourselves to the case $\ell = 0$, that is, the electron has no orbital angular momentum. To recast this equation into a simpler form, we'll define $\rho \equiv r/\alpha$ where α is some parameter with units length. Then eq. (8) can be rewritten as

$$-\frac{\mathrm{d}^2u(\rho)}{\mathrm{d}\rho^2}+\rho^2u(\rho) = \lambda u(\rho), \tag{9}$$

as derived in the section VI B 1. This can be recast into eq.(3) with

$$U_i = 2 + \rho_i^2, \qquad \forall i \in \{1, 2, ..., n\}. \tag{10}$$

The same Dirichlet boundary conditions is assumed here, $u(0) = 0$ and $u(\infty) = 0$. This assures that the resulting radial function obeys $\int r^2|R(r)|^2dr < \infty$ such that $R(r) \in L^2(0, \infty)$ and is thus normalisable.

The boundary condition $u(\infty) = 0$ raises a problem: we need to approximate infinity in our numerical calculation. The approximation, which we name $\rho_{\max}$, will depend on the natural length scale of the constant $\alpha = (\hbar/m\omega)^{1/2}$ (see section VI B 1). The goal is to tune $\rho_{\max}$ in such order that we obtain the first three eigenvalues with three leading digits. We want to investigate which $\rho_{\max}$ gives the best approximation to the analytical answer for the first four individual eigenvalues as well as the best overall approximation for the first four eigenvalues. As stepsize is a function of both $\rho_{\max}$ and n, changing either will have an impact on the precision of our result. We chose to use $n = 350$ and look at how the relative error in our computed eigenvalues changed when using different values for $\rho_{\max}$. From eq.(45), the analytical values for the first four eigenvalues are $\lambda_1 = 3, \lambda_2 = 7, \lambda_3 = 11, \lambda_4 = 15$.

D. Quantum dots in 3D - two electrons

The Schrödinger equation for two electrons with no repulsive Coulomb interactions reads

$$E^{(2)}u(r_1, r_2) =$$

$$\left(-\frac{\hbar^2}{2m}\frac{\mathrm{d}^2}{\mathrm{d}r_1^2}-\frac{\hbar^2}{2m}\frac{\mathrm{d}^2}{\mathrm{d}r_2^2}+\frac{1}{2}kr_1^2+\frac{1}{2}kr_2^2\right)u(r_1, r_2), \tag{11}$$

where $u(r_1, r_2)$ is the two-electron wave function and $E^{(2)}$ is the two-electron energy. This can be written as

$$E^{(2)}u(r,R) =$$

$$\left(-\frac{\hbar^2}{m}\frac{\mathrm{d}^2}{\mathrm{d}r^2} - \frac{\hbar^2}{4m}\frac{\mathrm{d}^2}{\mathrm{d}R^2} + \frac{1}{4}kr^2 + kR^2\right)u(r,R), \quad (12)$$

where we introduced the relative coordinate $\mathbf{r} = \mathbf{r}_1 - \mathbf{r}_2$ with the center-of-mass coordinate $\mathbf{R} = (\mathbf{r}_1 + \mathbf{r}_2)/2$ and $r \equiv \|\mathbf{r}\|$. The wave function is separable by $u(r,R) = \psi(r)\phi(R)$, and so the energy of the system is equal to the sum of relative energy E_r and the center-of-mass energy E_R

$$E^{(2)} = E_r + E_R. \quad (13)$$

Including the repulsive Coulomb interaction between two electrons [3], the radial part of the Schrödinger equation can be written as

$$\left(-\frac{\hbar^2}{m}\frac{\mathrm{d}^2}{\mathrm{d}r^2} + \frac{1}{4}kr^2 + \frac{\beta e^2}{r}\right)\psi(r) = E_r\psi(r), \quad (14)$$

with $\beta e^2 = 1.44$ eVnm. We want to recast this equation into a simpler form, as we did with the equation for the one electron problem. For this we introduce a dimensionless variable $\rho = r/\alpha$ and the equation we obtain is then

$$-\frac{\mathrm{d}^2}{\mathrm{d}\rho^2}\psi(\rho) + \omega_r^2\rho^2\psi(\rho) + \frac{1}{\rho}\psi(\rho) = \lambda\psi(\rho), \quad (15)$$

as derived in section VI B 2. This can easily be recast into eq.(3) with

$$U_i = 2 + \omega_r^2\rho_i^2 + \frac{1}{\rho_i}, \qquad \forall i \in \{1, 2, ..., n\}. \quad (16)$$

We will treat ω_r as a parameter which reflects the strength of the oscillator potential, and look at the following values for $\omega_r : 0.01, 0.5, 1.0$ and 5.0.

In the case where there is no repulsive Coulomb interaction, the eigenvalues will coincide with the relative energy of a non-interacting system. For specific oscillator frequencies eq. (15) has analytical answers, found in the article by M. Taut [11], so that the computed eigenvalues can be verified and assertion of the validity of our implementation can be justified. Finally we will analyze the dimensionless probability distribution for position, formally defined as $|\psi(\rho)|^2 = |\langle\rho|\psi\rangle|^2$ for different frequencies, with and without the repulsive Coulomb interaction between the two electrons. By comparison, these two cases are expected to display differing probability distributions $|\psi(\rho)|^2$. Specifically, we predict that expectation value $\langle\rho\rangle$ will tend to be higher for the case with electron-electron repulsion. This is a natural consequence, since the repulsive force will tend to push the electrons away from each others, which is simply a qualitative statement about $\langle\rho\rangle$. However, to reduce the necessary computations, we will qualitatively determine this by visualizing the probabilitity distributions themselves and take for granted that the maxima of these distributions are good indicators of the expectation values.

As in the one electron case, we are only interested in the ground state $\ell = 0$ and the same boundary conditions are valid, so the issue with $u(\infty) = 0$ still need to be resolved. We neglect the center-of-mass energy, and are only interested in the relative energy.

E. Algorithm

Jacobi's method is a approximation scheme designed to find the eigenvalues of a real symmetric matrix A through as series of similarity transformations $A' = S^T AS$, where S is a unitary matrix. Conceptually, the similarity transformation will gradually change the coordinate basis representation of A until it is represented with respect to a basis consisting of its own eigenvectors. At this point, A' will be a diagonal matrix with its eigenvalues on the diagonal.

In Jacobi's method, the unitary matrix S is a rotation matrix as follows.

$$S = \begin{bmatrix} 1 & \cdots & 0 & \cdots & 0 & \cdots & 0 \\ \vdots & \ddots & \vdots & & \vdots & & \vdots \\ 0 & \cdots & c & \cdots & s & \cdots & 0 \\ \vdots & & \vdots & \ddots & \vdots & & \vdots \\ 0 & \cdots & -s & \cdots & c & \cdots & 0 \\ \vdots & & \vdots & & \vdots & \ddots & \vdots \\ 0 & \cdots & 0 & \cdots & 0 & \cdots & 1 \end{bmatrix}, \quad (17)$$

where $c \equiv \cos\theta$ and $s \equiv \sin\theta$. Let s_{ij} denote the matrix elements of S. As a convention, we shall denote $s_{kk} = s_{ll} = c$, $s_{kl} = -s_{lk} = s$.

The similarity transformation $A' = S^T AS$ leads to the follwing equations (for an excellent review of these derivations, see [7][8]).

$$a'_{ii} = a_{ii}, \qquad i \neq k, i \neq l \quad (18)$$
$$a'_{ik} = a_{ik}c - a_{il}s, \quad i \neq k, i \neq l \quad (19)$$
$$a'_{il} = a_{il}c + a_{ik}s, \quad i \neq k, i \neq l \quad (20)$$
$$a'_{kk} = a_{kk}c^2 - 2a_{kl}cs + a_{ll}s^2 \quad (21)$$
$$a'_{ll} = a_{ll}c^2 + 2a_{kl}cs + a_{kk}s^2 \quad (22)$$
$$a_{kl} = (a_{kk} - a_{ll})cs + a_{kl}(c^2 - s^2). \quad (23)$$

We require that

$$a_{kl}(c^2 - s^2) + (a_{kk} - a_{ll})cs = 0, \quad (24)$$

which is tantamount to demanding that the non-diagonal elements are zero. Defining the quantities $\tan\theta \equiv t = s/c$ and

$$\tau = \frac{a_{ll} - a_{kk}}{2a_{kl}}, \quad (25)$$

we obtain the equation

$$t^2 + 2\tau t - 1 = 0, \tag{26}$$

with corresponding solutions

$$t = -\tau \pm \sqrt{1+\tau^2}. \tag{27}$$

From this we get obtain that

$$c = \frac{1}{\sqrt{1+t^2}}, \tag{28}$$

and $s = tc$.

Jacobi's method can thus be summarized as follows:

Algorithm 1 Jacobi's method

while $\max_{i\neq j} |A_{ij}|^2 \geq \epsilon$ **do**
  $a_{kl} = \max_{i\neq j} |A_{ij}|$
  if $a_{kl} \neq 0$ **then**
    $\tau = (a_{ll} - a_{kk})/2a_{kl}$
    if $\tau \geq 0$ **then**
      $t = 1/(\tau + \sqrt{1+\tau^2})$
    else
      $t = 1/(\tau - \sqrt{1+\tau^2})$
    $c = 1/\sqrt{1+t^2}$
    $s = ct$
  else
    $c = 1.0$
    $s = 0.0$
  $a'_{kk} = c^2 a_{kk} - 2csa_{kl} + s^2 a_{ll}$
  $a'_{ll} = s^2 a_{kk} + 2csa_{kl} + c^2 a_{ll}$
  $a_{lk} = a_{kl} = 0.0$
  for $i = 1, 2, .., n$ **do**
    if $i \neq k \ \wedge \ i \neq l$ **then**
      $a'_{ik} = ca_{ik} - sa_{il}$
      $a'_{ki} = a_{ik}$
      $a'_{il} = ca_{il} + sa_{ik}$
      $a_{li} = a_{il}$
$\lambda_i = a'_{ii}$

Let $I(n, \epsilon)$ be the number of iterations necessary for Jacobi's method to converge for a given tolerance ϵ and number of gridpoints n such that $A \in \mathbb{R}^{n\times n}$. For Jacobi's method, it's expected that $I(n, \epsilon) \propto n^2$ for reasonably small ϵ. [9]

F. Important mathematical properties

1. Unitary transformations conserve orthonormality

Suppose A is a symmetric matrix and S is a unitary matrix, such that $S^\dagger S = SS^\dagger = 1$. Suppose further that $\{\boldsymbol{v}_i\}$ are a orthonormal set of eigenvectors of A. It then follows that

$$\begin{aligned}\langle S\boldsymbol{v}_i, S\boldsymbol{v}_j\rangle = (S\boldsymbol{v}_i)^\dagger (S\boldsymbol{v}_j) = \boldsymbol{v}_i^T (S^\dagger S)\boldsymbol{v}_j \\ = \langle \boldsymbol{v}_i, \boldsymbol{v}_j\rangle = \delta_{ij},\end{aligned} \tag{29}$$

where δ_{ij} is the Kronecker delta.

2. Similar matrices share eigenvalue spectrum

Suppose B is similar to A, that is $B = S^T AS$ for a real unitary matrix S. We prove here that B has the same eigenvalues as A. Let $\boldsymbol{v}_i$ have the corresponding eigenvalue λ_i, then

$$B(S^T\boldsymbol{v}_i) = S^T A\boldsymbol{v}_i = \lambda_i(S^T\boldsymbol{v}_i), \tag{30}$$

which proves that B has eigenvalues λ_i with corresponding eigenvectors $S^T\boldsymbol{v}_i$.

3. The eigenvectors of a similar matrix are orthogonal

Suppose $B = S^T AS$ and A is symmetric, then

$$B^T = \left(S^T AS\right)^T = S^T A^T (S^T)^T = S^T AS = B, \tag{31}$$

By the spectral theorem for symmetric matrices, it follows that the eigenvectors of B residing in different eigenspaces are orthogonal.

In our numerical calculations for finding the eigenpairs, the three mathematical properties above are all tested to ensure that the these are obeyed.

G. Relative error

In this article we define the relative error as

$$\epsilon_{\text{rel}} = \frac{|\lambda_c - \lambda_a|}{\lambda_a}, \tag{32}$$

where λ_c and λ_a refers to the computed and analytically obtained eigenvalues, respectively. We similarly define the total relative error as

$$E_{\text{rel}} = \sum_j \frac{\left|\lambda_j^c - \lambda_j^a\right|}{\lambda_j^a}, \tag{33}$$

where λ_j^c and λ_j^a refers to the j-th computed and analytical eigenvalue, respectively. The superscripts a and c are just labels and should not be confused with exponents.

III. RESULTS

The results described in this section where all computed using a tolerance of $\epsilon = 10^{-12}$ as described in algorithm 1.

A. The Jacobi method's performance

We measured the time the Jacobi method used to compute the eigenvalues in the buckling beam problem

for different matrix dimensions, and compared it to Armadillo's library function *eig_sym* [4]. The result is displayed graphically in FIG. 1.

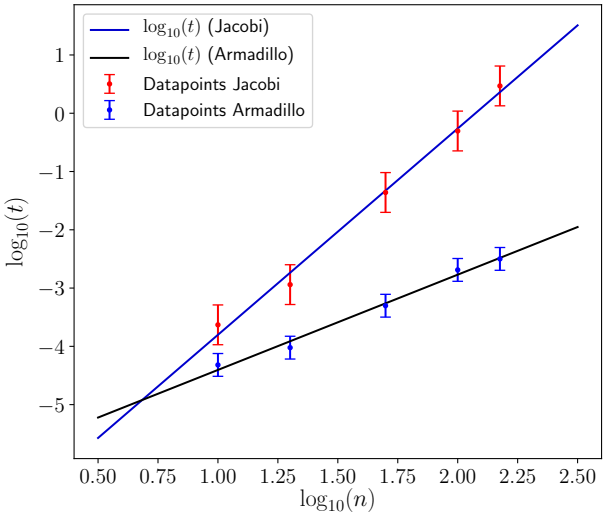

FIG. 1. Comparison of time used for computing eigenvalues for the Jacobi method and Armadillo's library function *eig_sym*, for the buckling beam problem. n is the number of grid points and t is the time used.

The error bars are given by the standard deviation obtained from the linear regression of the data points using the method of least squares as described here [10]. The functions shown in FIG. 1 are

$$\log_{10}(t) = (3.54 \pm 0.17)\log_{10}(n) - 7.34 \pm 0.29 \quad (34)$$
$$\log_{10}(t) = (1.63 \pm 0.09)\log_{10}(n) - 6.03 \pm 0.16, \quad (35)$$

where eq. (34) and (35) is a representation of the computed time used by Jacobi's method and Armadillo, respectively. From this, we can extract that

$$t_{\text{Jacobi}} \propto n^{3.54\pm0.17} \quad (36)$$
$$t_{\text{Armadillo}} \propto n^{1.63\pm0.09}. \quad (37)$$

The number of iterations needed to reach convergence $I(n)$ was computed for several choices of n. The results are represented in FIG. 2

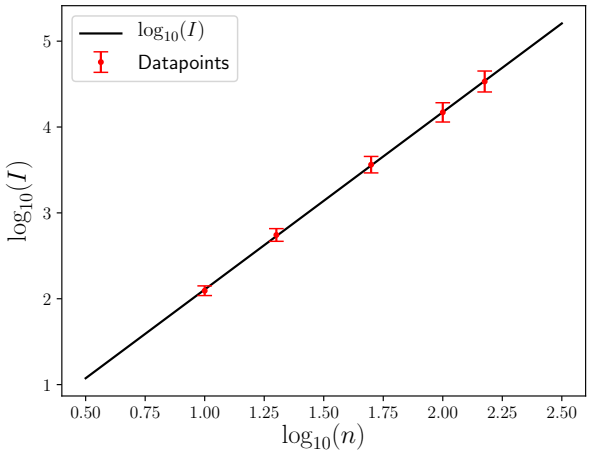

FIG. 2. The figure shows the logarithm of the number of iterations needed to reach convergence $\log_{10}(I)$ as function of the number of gridpoints n. This was computed by solving the DE modelling the buckling beam problem. The tolerance was chosen to be $\epsilon = 10^{-12}$.

The function represented is

$$\log_{10}[I(n)] = (2.066 \pm 0.013)\log_{10}(n) + (0.04 \pm 0.02),$$

from which we can deduce that

$$I(n) \propto n^{2.066\pm0.013} \quad (38)$$

B. A Buckling Beam problem

Implementing Jacobi's method to solve the buckling beam problem works as a stepping stone towards more complex issues. The only result we generated, along with testing the Jacobi algorithms efficiency against Armadillo, were the eigenvalues of the matrix in eq. (3), with $U_i = 2$. The eigenvalues will converge to the true eigenvalues, which can be found analytically (see section VI A for derivation), for higher values of n. FIG. 3 illustrates the relation between the relative error for λ_i for $i = 2, 3, 4$ and the number of grid points n.

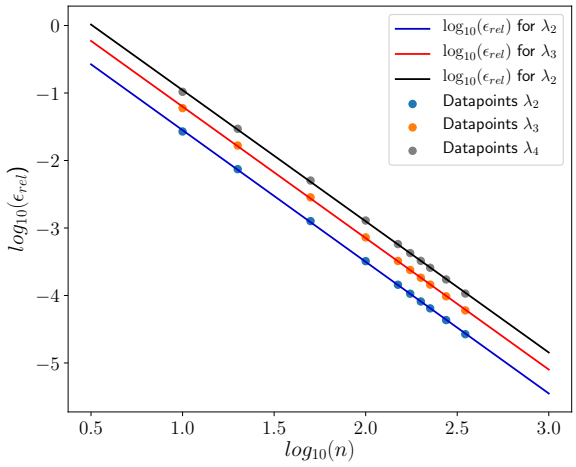

FIG. 3. Relative error (ϵ_{rel}), as a function of number of grid points n, in the computed eigenvalues for λ_i for $i = 2, 3, 4$. This was done using the closed-form solution of the spectrum in eq. (7) and the approximated eigenvalues obtained with Jacobi's method.

The functions show in FIG. 3 are obtained with the same method as those in FIG. 1.

$$\log_{10}[\epsilon_{\text{rel}}(n)] = (-1.950 \pm 0.007)\log_{10}(n) + (0.400 \pm 0.015)$$
$$\log_{10}[\epsilon_{\text{rel}}(n)] = (-1.947 \pm 0.008)\log_{10}(n) + (0.746 \pm 0.016)$$
$$\log_{10}[\epsilon_{\text{rel}}(n)] = (-1.943 \pm 0.009)\log_{10}(n) + (0.986 \pm 0.018)$$

From the equations above the following relation becomes evident

$$\epsilon_{\text{rel}} \underset{\sim}{\propto} n^{-2} \tag{39}$$

C. Quantum dots in 3D - one electron

We looked at the 4 first eigenvalues/energies for a span of several $\rho_{\max}$ and compared the computed results to the analytical eigenvalues by looking at relative error. The plot of error vs. $\rho_{\max}$ for each of the four eigenvalues is presented in figure 4. We also summed the relative errors for all four and looked at total error vs. $\rho_{\max}$. This is presented in figure 5. From the total error figure we see that the $\rho_{\max}$ that gives the lowest relative error from the analytical was $\rho_{\max} = 5.20$. The first four computed eigenvalues for the $\rho_{\max}$ that gave the highest accuracy for each of them are presented in table I.

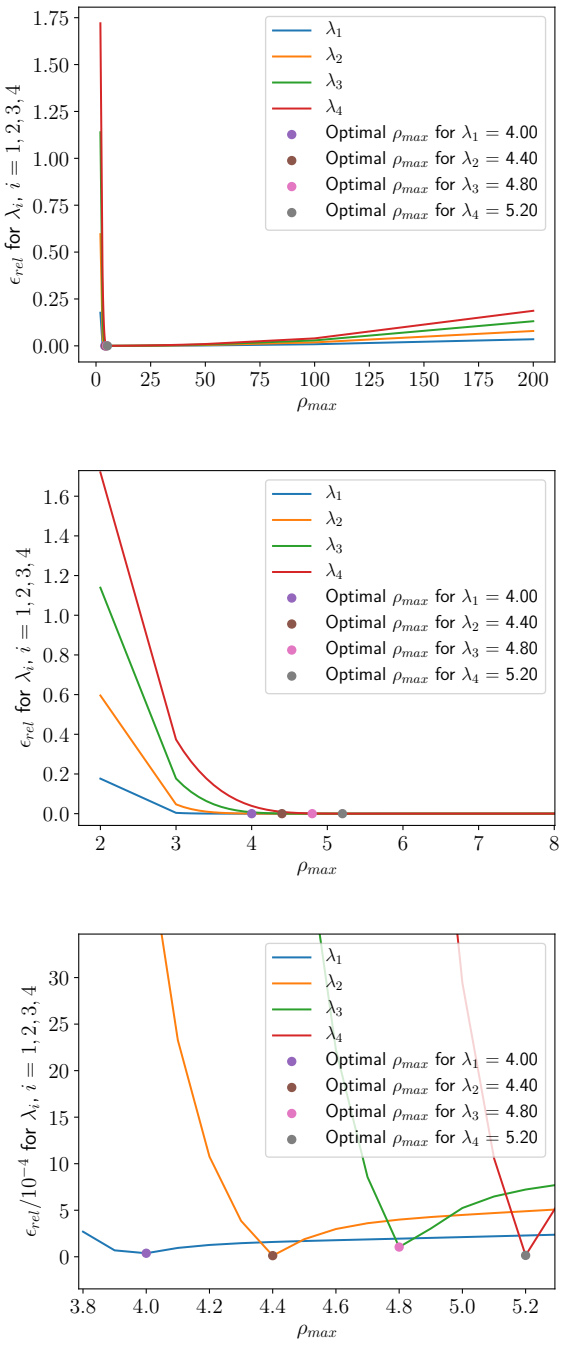

FIG. 4. The figures show the relative error ϵ_{rel} for λ_i for $i = 1, 2, 3, 4$ pertaining to the approximated spectrum of the differential operator of the 3-dimensional HO with one electron. The figure on top displays the overall tendency of the relative error while the two others are zoomed in and show the optimal choices of $\rho_{\max}$ for each eigenvalue.

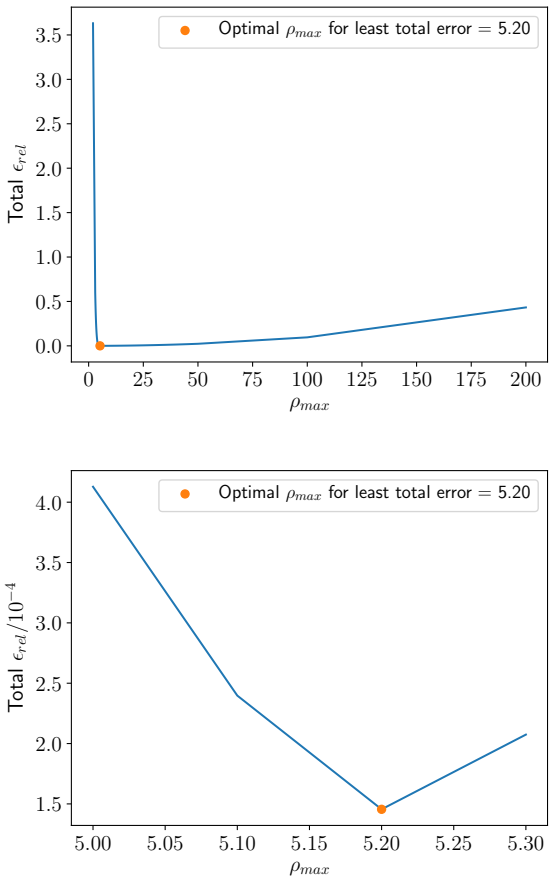

FIG. 5. The figures shows the total relative error as a function of $\rho_{\max}$. It is computed using the approximated spectrum of the differential operator of the 3-dimensional HO and the analytical values. The figure on top shows the overall total relative error, while the bottom figure is zoomed in on the area at which the global minimum occurs. This corresponds to the optimal choice of $\rho_{\max}$.

$\rho_{\max}$	λ_1	λ_2	λ_3	λ_4
4.00	2.99998	7.00317	11.07831	15.58610
4.40	2.99995	7.00000	11.00971	15.13502
4.80	2.99994	6.99972	11.00011	15.01777
5.20	2.99993	6.99965	10.99920	15.00002

TABLE I. The table shows the four lowest eigenvalues computed for the 3-dimensional HO with one electron with several different values of $\rho_{\max}$.

D. Quantum dots in 3D - two electrons

The ground state eigenvalue of (15) was computed for three different ω_r's. These parameters were chosen such that comparison with the analytical values found in M. Taut's article [11]. The analytical values in this article is given as $\epsilon' = \lambda/2$. The result is shown in table II.

$1/\omega_r$	$\epsilon' = \lambda/2$	ϵ	$\lvert\epsilon' - \epsilon\rvert/\epsilon$ [%]
4	0.6248	0.6250	3.2×10^{-2}
20	0.1750	0.1750	0
115.299	0.0502	0.0477	5.2

TABLE II. The computed ground state eigenvalues shown with the analytical results extracted from [11] for three different ω_r's. The computations were done with $n = 200$ and $\rho_{\max} = 30$.

The ground state wavefunctions, both for the case of repulsion and no repulsion, were computed using armadillo.

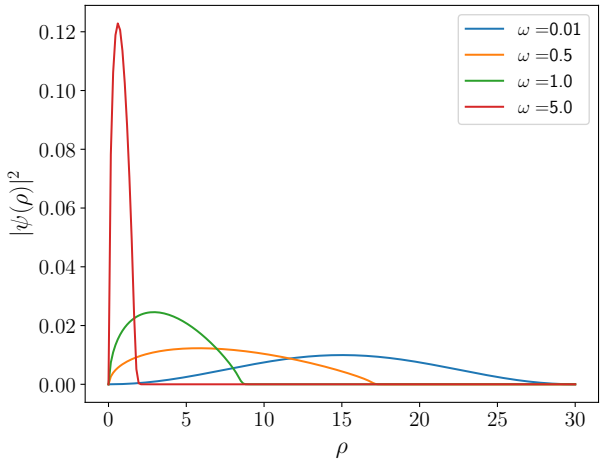

FIG. 6. The probability distribution $|\psi(\rho)|^2$ for the case without electron-electron repulsion for $\omega_r = 0.01, 0.5, 1.0, 5.0$. We used the following parameters: $\rho_{\max} = 30$ and $n = 200$.

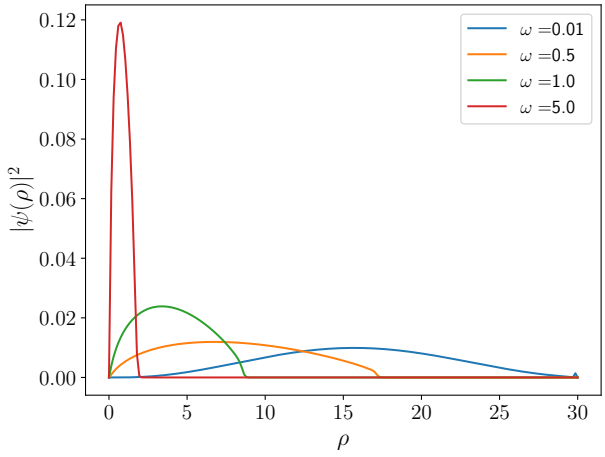

FIG. 7. The probability distribution $|\psi(\rho)|^2$ for the case with electron-electron repulsion for $\omega_r = 0.01, 0.5, 1.0, 5.0$. The parameters used were $\rho_{\max} = 30$ and $n = 200$.

IV. DISCUSSION

A. Convergence rate of Jacobi's method

We expected that the number of iterations required by Jacobi's method to reach convergence for a reasonably small tolerance was $I(n) \propto n^2$. From the data represented in FIG 2, we found that $I(n) \propto n^{2.066\pm0.013}$. Clearly, the computations are in agreement with the quadratic convergence rate shown here [6], essentially confirming that the algorithm is implemented correctly. The slight deviation from n^2 could possibly be explained by our choice of tolerance ϵ. In our analysis, we've assumed that the dependence on choice of tolerance is virtually non-existent - aside from demanding it to be reasonably (and vaguely so) small - and suggest that to scrutinizing this dependency in more detail is a fruitful topic for further investigation.

We can note that from the computed time used, Jacobi's method obeys roughly $t \propto n^{3.54}$. In comparison with Armadillo's solver *eig_sym*, our implementation is substantially slower, so a natural prospective project would therefore be to optimize our code such that we can reduce the proportionality relation between t and n. If the optimization does not yield a better relationship than the eigenvalue solver, then we suggest other methods are better versed for the problems in this article.

B. The relative error

From FIG. 3, it is conspicuous that the number of grid points n is crucial in attaining the correct eigenvalues. The relative error goes approximately as the reciprocal of n^2, so the mathematical error is greatly reduced by increasing n. However, once n is increased sufficiently, it is expected that the error due to machine precision will dominate. However, in our computations, increasing n to the necessary order of magnitude isn't feasible on the computers used in this experiment as the RAM used on our computers are merely 16GB. A possible solution is to rewrite the code such that matrices aren't used, but instead the needed values are stored dynamically and deleted once their purpose is served. Otherwise, a supercomputer facility is necessary to test the expected dominance of machine precision due to the excessive working memory that's needed. We conclude that our computations here can be viewed as an experimental result. We propose that researching the mathematically predicted error to compare with the observed proportionality may gain further insight into Jacobi's method.

C. Optimal choice of $\rho_{\max}$

We observe that the best $\rho_{\max}$ for the smallest total error is not the same as best $\rho_{\max}$ for the individual eigenvalues, as they differ which we clearly see from figure 4. We observe that our computed values for the lower eigenvalues are most accurate when we use a small value for $\rho_{\max}$, and that our computed values for the larger eigenvalues are most accurate when we use a higher $\rho_{\max}$. We can see from table I that while the lowest eigenvalue only has a loss of accuracy in its fifth digit after the decimalpoint for larger values of $\rho_{\max}$, the highest has a change in its first. This means that the gain in accuracy is much larger for λ_4 than the loss of accuracy is for λ_1 when changing the value of $\rho_{\max}$ slightly. From this we expected that the $\rho_{\max}$ that gives the lowest total relative error would be closer to the $\rho_{\max}$ which gives the lowest relative error in λ_4 than the $\rho_{\max}$ which gives the lowest relative error in λ_1. This coheres well with our finding that the optimal $\rho_{\max}$ for least total error was not only close to, but the same as the optimal $\rho_{\max}$ for least error in λ_4.

Had we looked at how the accuracy of the larger eigenvalues, say λ_{200}, changed with different values of $\rho_{\max}$, we would expect them to follow the same pattern as the first four. As seen from figure 4, the larger the eigenvalue is, the less steep the error curve for that eigenvalue is beyond is global minimum. That is to say that we, based on our results, can extrapolate that the convexity of the error curve for larger values of λ are smaller than the convexity of the error curve for smaller values of λ. The step size is a function of both n and $\rho_{\max}$, $h = (\rho_{\max} - \rho_{\min})/n$, so for a given n the step size will increase for large values of $\rho_{\max}$ and decrease for small. But from the extrapolation above, we can infer that a larger step size won't put us that far from the accurate value for large values of λ. The problem will then be for the small values of λ who's error curves have higher convexity, where you can risk missing the mark substantially. Then again, for smaller values of $\rho_{\max}$, you risk cutting the function too short. That's to say you will never get the chance to get to the most accurate value for a large λ. This implies that perhaps the best method for computing eigenvalues is to look at which $\rho_{\max}$ gives the most accurate value for the individual eigenvalues and using those results instead of a universal $\rho_{\max}$. Finding the optimal $\rho_{\max}$ for the first four eigenvalues demanded extensive work, so estimating it for all 350 would require a considerable amount of time. The error plots would also be quite unreadable and hard to extract relevant information from, which is why we decided to only look at the first four. This could be an interesting topic to explore more thoroughly, but as a project on its own entirely.

D. The computed ground state wavefunctions

When the strength of the HO potential decreases we would expect the probability distribution $|\psi|^2$ to widen and vice versa for increasing ω_r. Stronger potential generates a stronger force exerted on the electrons, so the distance between them will statistically be smaller. We

would therefor expect the probability distribution to be steeper and narrower for higher ω_r. Figures 6 and 7 clearly exhibit these theoretical properties.

In the case where there is no repulsion between the electrons, the predicted expectation values would be higher than in the case with repulsion for obvious reasons. At first glance the two figures look approximately equal to one another, but by looking at the maxima for the different values of ω_r, a tiny variation becomes evident. The maximum values are somewhat higher in the no-repulsion case. For $\omega_r = 5.0$ when there is no repulsion the max. value is < 0.12, but > 0.12 when the electron-electron repulsion is present. Since the probability distribution is normalized, the area below the curves in both figures are fixed. The change in expectation value is therefor coherent with the theoretical prediction.

E. Computed ground state eigenvalues

In table II, the relative error has an apparent erratic nature, but this is a result of the restrictive number of digits presented in M. Taut's article. Nevertheless, our computed ground state eigenvalues are of the same order of magnitude as the analytical ones.

Although the computed eigenvalues is somewhat consistent with the analytical values, it is clear that one should perform the computations for more ω_r's and several different n's and $\rho_{\max}$'s. We suggest, therefore, that a prospective topic of investigation is to compute the eigenvalues for a wider range of these parameters and compare with the ones obtained analytically.

V. CONCLUSION

In this article we've studied how certain DEs modelling physical problems that inherently are eigenvalue problems can be scaled and recast into matrix equations by discretization. We defined an approximate mapping from the differential operator acting on the infinite-dimensional operator onto an approximate finite-dimensional operator represented by a matrix. We then solved the resulting approximate eigenvalue equation by Jacobi's method.

We studied how the number of iterations necessary to reach convergence $I(n)$ depended on the number of grid points n and found that $I \propto n^{2.066\pm0.013}$ which is in agreement with the predicted convergence rate found in the literature. Furthermore, we studied the time used by Jacobi's method as a function of n and found that $t_{\text{Jacobi}} \propto n^{3.54\pm0.17}$. We found that the eigenvalue solver *eig_sym* from Armadillo displayed $t_{\text{Armadillo}} \propto n^{1.63\pm0.09}$, thus being a much faster solver. We therefore conclude that our implementation is in serious need of optimization, should it be preferred over this fast eigenvalue solver.

The relative error ϵ_{rel} between the approximated eigenvalues and the analytical ones display a dependency $\epsilon_{\text{rel}} \propto n^{-2}$, which we take as an experimental result that should be studied theoretically from a mathematical point of view. Due to the limited working memory on the computers used in our simulations, we could not provide sufficient data to esimate the optimal choice of n nor any data on how the error behaves once the error due to machine precision begins to dominate. We suggest therefore that further investigations into these areas may be fruitful to understand the efficacy of Jacobi's algorithm better.

We studied which optimal choice of $\rho_{\max}$ was needed to produce the four lowest eigenvalues, and found that each eigenvalue require a corresponding optimal maximum value of ρ in order to yield the lowest relative error. The total relative error overall is much more complicated as this optimal $\rho_{\max}$ depend of the number of grid points n we choose to study the problem with. When we determined which $\rho_{\max}$ we ideally should choose in each case, we restricted ourselves to fix $n = 350$, so our dataset is somewhat limited of value and here we conclude that one should perform a more thorough analysis in order to gain conclusive insight into this dependency.

We looked at how we could solve the radial equation obtained from quantum mechanical models for a three dimensional harmonic oscillator by application of Jacobi's algorithm. The computed ground state wavefunctions gave rise to probability distributions that qualitatively adhered with the predicted behaviour. With inclusion of electron-electron repulsion, we observed that maxima had a tendency to be shifted toward higher values of ρ than when this physical process was neglected. Furthermore we found that the distributions had a narrower peak for larger values of ω_r. To improve this analysis, the expectation values $\langle\rho\rangle$ of the distributions should be computed and a comparison between the inclusion and exclusion of electron-electron repulsion can be done to clearly demonstrate the predictions.

As a final remark, we think that this article has presented a method for solving DEs that works, but is in itself not a particularly efficient implementation. Unless it is optimized in an ingenious way, one is better off using other methods or eigenvalue solvers such as *eig_sym* from Armadillo for these type of problems.

VI. APPENDIX

A. Eigenvalues of the Buckling Beam problem

The DE

$$-\frac{\mathrm{d}^2u(\rho)}{\mathrm{d}\rho^2} = \lambda u(\rho), \tag{40}$$

has the general solution

$$u(\rho) = A\cos\left(\sqrt{\lambda}\rho\right) + B\sin\left(\sqrt{\lambda}\rho\right). \tag{41}$$

The boundary conditions $u(0) = u(1) = 0$ implies

$$u(0) = A = 0, \tag{42}$$

and

$$u(1) = B\sin\sqrt{\lambda} = 0, \tag{43}$$

yielding the eigenspectrum

$$\lambda_n = \pi^2 n^2, \qquad n = 0, 1, 2, ... \tag{44}$$

B. Scaling the Schrödinger Equation

1. One electron

To obtain eq. (9) we introduce the dimensionless variable $\rho \equiv r/\alpha$, where α is an arbitrary constant with the same dimension as r. Eq. (8) is the radial equation for any spherically symmetric potential $V(r)$, but in our case $V(r)$ is the potential of a harmonic oscillator (HO) with $\ell = 0$. Eq. (8) now reads

$$-\frac{\hbar^2}{2m}\frac{\mathrm{d}^2u(r)}{\mathrm{d}r^2} + \frac{1}{2}kr^2u(r) = Eu(r),$$

where $k = m\omega^2$ and E is the energy for the HO in three dimensions. The energy depends on the frequency ω and the quantum numbers n and ℓ.

$$E_{n\ell} = \hbar\omega\Big(2n + \ell + \frac{3}{2}\Big),$$

with $n = 0, 1, 2, ...$ and $\ell = 0, 1, 2, ...$; By inserting the new variable ρ, along with the chain rule, we obtain the following equation:

$$-\frac{\hbar^2}{2m\alpha^2}\frac{\mathrm{d}^2u(\rho)}{\mathrm{d}\rho^2} + \frac{1}{2}m\omega^2\alpha^2\rho^2u(\rho) = Eu(\rho) \quad \Big| \cdot \frac{2m\alpha^2}{\hbar^2}$$

$$-\frac{\mathrm{d}^2u(\rho)}{\mathrm{d}\rho^2} + \frac{m^2\alpha^4\omega^2}{\hbar^2}\rho^2u(\rho) = \frac{2m\alpha^2E}{\hbar^2}u(\rho)$$

To eradicate the quotient in the central term we set a natural length scale on the constant α, where α now equals $(\hbar/m\omega)^{1/2}$. By defining $2m\alpha^2E/\hbar^2 \equiv \lambda$, we end up with eq. (9). From this it follows that

$$\lambda_n = 4n + 3, \qquad n = 0, 1, 2, ... \tag{45}$$

2. Two electrons

When introducing the dimensionless variable ρ we can rewrite eq. (14) as

$$-\frac{\mathrm{d}^2}{\mathrm{d}\rho^2}\psi(\rho) + \frac{1}{4}\frac{mk}{\hbar^2}\alpha^4\rho^2\psi(\rho) + \frac{m\alpha\beta e^2}{\rho\hbar^2}\psi(\rho) = \frac{m\alpha^2}{\hbar^2}E_r\psi(\rho).$$

To simplify even further we define oscillator frequency ω_r as

$$\omega_r^2 = \frac{1}{4}\frac{mk}{\hbar^2}\alpha^4,$$

while requiring

$$\alpha = \frac{\hbar^2}{m\beta e^2}.$$

Lastly, if we define

$$\lambda = \frac{m\alpha^2}{\hbar^2}E,$$

we can write the Schrödringer equation in its final form as

$$-\frac{\mathrm{d}^2}{\mathrm{d}\rho^2}\psi(\rho) + \omega_r^2\rho^2\psi(\rho) + \frac{1}{\rho} = \lambda\psi(\rho). \tag{46}$$

[1] http://arma.sourceforge.net/docs.html.
[2] https://github.com/reneaas/ComputationalPhysics/tree/master/projects/project2.
[3] https://github.com/CompPhysics/ComputationalPhysics/blob/master/doc/Projects/2019/Project2/pdf/Project2.pdf.
[4] http://arma.sourceforge.net/docs.html#eig_sym.
[5] Darrel F. Schroeter David J. Griffiths. *Introduction to Quantum Mechanics, 3rd ed.*, chapter 4.1, pages 138–139. 2018.
[6] Charles F. Van Loan Gene H. Golub. *Matrix Computations*, chapter 8.5.3, page 479. 2013.
[7] Charles F. Van Loan Gene H. Golub. *Matrix Computations 4th ed.* 2013.
[8] Morten Hjorth-Jensen. *Computational Physics, Lecture Notes Fall 2015.* 2015.
[9] Morten Hjorth-Jensen. *Computational Physics, Lecture Notes Fall 2015*, chapter 7.4, page 217. 2015.
[10] G.L Squires. *Practical Physics, 4th ed.*, chapter 4.4, page 39. 2001.
[11] M. Taut. Two electrons in an external oscillator potential: Particular analytic solutions of a coulomb correlation problem. *Physical Review A*, 1993.